Real-space renormalization group study of the anisotropic antiferromagnetic Heisenberg model of spin $S = 1$ on a honeycomb lattice

2005 J. Phys.: Condens. Matter 17 1769

(http://iopscience.iop.org/0953-8984/17/12/001)

INSTITUTE OF PHYSICS PUBLISHING JOURNAL OF PHYSICS: CONDENSED MATTER

J. Phys.: Condens. Matter **17** (2005) 1769–1780 doi:10.1088/0953-8984/17/12/001

Real-space renormalization group study of the anisotropic antiferromagnetic Heisenberg model of spin $S = 1$ on a honeycomb lattice

A S Boyarchenkov[1], A S Ovchinnikov[1,4], I G Bostrem[1], N V Baranov[1], Y Hosokoshi[2] and K Inoue[3]

[1] Department of Physics, Ural State University, 620083, Ekaterinburg, Russia
[2] Osaka Prefecture University, Osaka 599-8531, Japan
[3] Department of Chemistry, Hiroshima University, Hiroshima 739-8526, Japan

Received 19 January 2005
Published 11 March 2005
Online at stacks.iop.org/JPhysCM/17/1769

Abstract

The real-space renormalization group approach is applied to study critical temperatures of a system consisting of interacting spin chains of spin $S = 1$, with an inner antiferromagnetic exchange, which form a honeycomb crystal lattice. Using the anisotropic Heisenberg model we calculate the critical temperature as a function of the anisotropic parameter and the ratio of the interchain and intrachain interactions. A comparison our results with those obtained from RSRG calculations for the same model of spin-1/2 on a square lattice is given.

1. Introduction

The study of low-dimensional magnetic systems made of spin chains has attracted much attention over the last few decades. If the interchain coupling is less than intrachain one, at higher temperatures these systems exhibit properties intrinsic to one-dimensional magnets. However, at lower temperatures the interchain interaction comes into play and begins to govern the magnetic behaviour of the system.

In this work we apply the real-space renormalization group (RSRG) procedure to the antiferromagnetic Heisenberg model of spin $S = 1$ on a honeycomb lattice made of antiferromagnetic spin $S = 1$ chains with antiferromagnetic interchain coupling. We are interested in the critical properties of the 2D system, and explore how the interchain coupling affects the criticality of the model. Simultaneously, we elucidate the effect of exchange anisotropy on the critical temperature and build the phase diagram of the anisotropic Heisenberg (AH) model of spin $S = 1$ on a honeycomb lattice with two kinds of exchange coupling.

First of all, the interest in the problem is motivated by the synthesis of a family of related organic biradicals PNNNO, PIMNO and F_2PNNNO whose magnetic properties have been

[4] Author to whom any correspondence should be addressed.

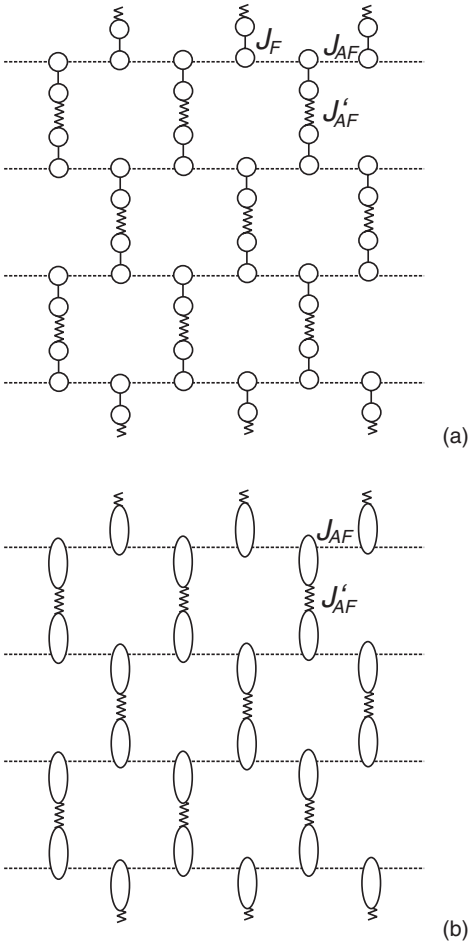

Figure 1. The magnetic model for F_2PNNNO. (a) Uniform chains with intramolecular ferromagnetic coupling (J_F) and intrachain antiferromagnetic coupling (J_{AF}). The chains interact antiferromagnetically (J'_{AF}). (b) The extreme limit of the model when $J_F \to \infty$: antiferromagnetic honeycomb lattice with $S = 1$.

examined by susceptibility and magnetization measurements [1]. Each biradical involves two spins of $S = 1/2$, which are coupled ferromagnetically (J_F). In their turn, these spin pairs couple antiferromagnetically in the crystal. Due to the strong ferromagnetic coupling J_F, antiferromagnetic chains of $S = 1$ are seen in both PNNNO and F_2PNNNO (see figure 2(a) type-I in [1]). PNNNO has interchain interactions in three-dimensions (3D), whereas F_2PNNNO has two-dimensional (2D) interchain interactions. PNNNO is well understood using the one-dimensional antiferromagnetic chain model. The compound undergoes 3D Néel order at $\sim$1 K due to weak interchain coupling. The crystal structure of F_2PNNNO is shown in figure 1. In the extreme limit of $J_F \to \infty$, the model becomes equivalent to the coupled antiferromagnetically (J'_{AF}) antiferromagnetic uniform chains of $S = 1$ with the intrachain exchange integral J_{AF}. F_2PNNNO, with comparable values of two kinds of antiferromagnetic interaction J_{AF} and J'_{AF}, forms a 2D system on a honeycomb lattice. It has been found that magnetism of F_2PNNNO is characterized by the singlet ground state and an

energy gap above the state. This finding is supported by the high-field magnetization process which shows a plateau in the magnetization curve. We have to point out that modelling of a real spin-1/2 system by a spin-1 system implies some mistake and one has to apply the results of the RSRG analysis to the real compounds with caution.

The results for the spin-1 lattice may also be useful for the theory of $S = 1$ bosons (ultracold atoms ^{23}Na) trapped in an optical lattice in the regime of one particle per site for suitable interaction between the bosons [2, 3].

According to recent quantum Monte Carlo results for spin-1/2 weakly anisotropic antiferromagnets on the square lattice, an ordered low-temperature phase develops for very small anisotropy of the order of 10^{-3}–10^{-2} (in units of exchange coupling) [4]. These results are in contradiction to the RSRG treatment for the same model predicting considerably larger value of the critical anisotropy ($\sim$0.2). In view of this discrepancy, the RSRG analysis for the $S > 1/2$ case is of particular theoretical interest and it is instructive to compare the critical behaviour of systems of integer and half-integer spins.

After the RSRG approach had been applied successfully to studying the 2D Ising systems [5, 6] a number of works were dedicated to the investigation of phase transitions in quantum systems within the method [7–9]. In last decade, RSRG methods have been performed to calculate the phase diagram for the anisotropic antiferromagnetic Heisenberg model of $S = 1/2$ on the square lattice [10, 11]. This approach uses a hierarchical lattice to approximate the square one, and performs a partial trace over internal degrees of freedom. Recently, in order to study weakly interacting classical and quantum spin chains, the linear-perturbation real-space renormalization group (LPRG) method has been suggested [12]. The LPRG uses the existence of the small parameter—the ratio of interchain to intrachain coupling. This perturbative method involves RG transformation, which for the Ising spins is the standard decimation procedure, and for the quantum spins is the generalization of the Suzuki–Takano approximate decimation [13]. However, in practice, the LPRG, using perturbation theory with the interchain interactions as the perturbation parameters, is only reliable for small values of the ratio interchain to intrachain interaction.

We use an extension to the $S = 1$ case of the quantum RSRG approach originally suggested by Mariz *et al* for the $S = 1/2$ AH model [14]. An application of the renormalization group method to interacting quantum spin chains encounters standard difficulties connected with the necessity for decomposition of the exponential operators, and additional proliferation of the new interactions due to the vector character of the spin operators.

The paper is organized as follows. In section 2 the RSRG method is formulated for $S = 1$ and applied to the honeycomb lattice formed by interacting antiferromagnetic chains. Our results and conclusions are given in section 3.

2. Model

We consider a system (anisotropic Heisenberg model) whose dimensionless Hamiltonian is defined by

$$-\beta H = \sum_{\langle i,j\rangle} K_{ij}\left[(1-\Delta_{ij})\left(S_i^x S_j^x + S_i^y S_j^y\right) + S_i^z S_j^z\right] \tag{1}$$

where $\beta = 1/k_{\mathrm{B}}T$, $K_{ij} \equiv J_{ij}/k_{\mathrm{B}}T$, J_{ij} is the exchange coupling constant, $\langle ij\rangle$ denotes first-neighbouring lattice sites, Δ_{ij} is the anisotropic parameter, and $S_i^{\alpha}\{\alpha = x, y, z\}$ is the spin-1 on the site i. The Hamiltonian (1) describes the Ising ($\Delta_{ij} = 1$), isotropic Heisenberg ($\Delta_{ij} = 0$) and XY-model ($\Delta_{ij} = -\infty$).

We mention briefly the main operations which are the basis of the approach of [14]. A parallel array of two bonds characterized respectively by (K_1, Δ_1) and (K_2, Δ_2) is equivalent to a single bond characterized by (K_p, Δ_p) given by

$$K_p = K_1 + K_2,$$
$$K_p\Delta_p = K_1\Delta_1 + K_2\Delta_2.$$

The extension of the approach, that is nothing but Migdal–Kadanoff procedure [15, 16], to n parallel bonds is straightforward.

For a series array of two bonds characterized by (K_1, Δ_1) and (K_2, Δ_2) the procedure involves difficulties due to non-commutativity effects. Under rescaling and removal of intermediate spins (decimation), the Hamiltonian changes and is characterized by a new set of parameters that are functions of the original set. The initial Hamiltonian is given by

$$H_{123} = K_1\left[(1-\Delta_1)\left(S_1^xS_3^x + S_1^yS_3^y\right) + S_1^zS_3^z\right] + K_2\left[(1-\Delta_2)\left(S_3^xS_2^x + S_3^yS_2^y\right) + S_3^zS_2^z\right].$$

We have to replace this array by a single bond whose Hamiltonian is

$$H'_{12} = K_s\left[(1-\Delta_s)\left(S_1^xS_2^x + S_1^yS_2^y\right) + S_1^zS_2^z\right] + K'_0. \tag{2}$$

We impose the preservation of the partition function between terminal sites 1 and 2, i.e.

$$\exp H'_{12} = \mathrm{Tr}_3 \exp H_{132}, \tag{3}$$

where Tr_3 denotes the tracing operation over the states of the intermediate spin-3, K'_0 is an additive constant included to make equation (3) possible. Equation (3) establishes the relation between the set of parameters (K_1, Δ_1), (K_2, Δ_2) and the set of renormalized parameters (K_s, Δ_s, K'_0). For the anisotropic spin-1/2 Heisenberg model corresponding expressions may be found explicitly [14, 10].

In order to construct recursion relations of the RG transformation (3) for the spin-1 model we should expand both sides over an appropriate matrix basis to equate the coefficients of the expansion. To avoid a proliferation problem we chose those quantities that correspond to coupling constants in the initial Hamiltonian (1).

Due to the properties of Pauli matrices the matrix representation for H and $\exp H$ in the case of spin-1/2 has the same form, i.e. H and $\exp H$ have non-zero matrix elements in the same positions. For $S = 1$ this rule does not hold, which results in an essential complication of the RG procedure.

Following the treatment of [14], we expand $\exp H'_{12}$ as

$$\exp H'_{12} = \sum_{n_1=0}^{\infty}\sum_{n_2=0}^{\infty} K_{n_1n_2}A_1^{n_1} \otimes A_2^{n_2},$$

where $\otimes$ is the outer product, $A_{1,2}$ are the ordinary powers of the spin operators $S_{1,2}^{x,y,z}$ and the coefficients $K_{n_1n_2}$ depend on K_s, Δ_s and K'_0. Since $A_{1,2}^n$ are the 3×3 matrices we expand them over the basis that consists of the polarization matrices T_q^k ($k = 0, 1, 2$ and $q = -k, -k+1, \ldots, k$) (see appendix A)

$$A_i^n = a\,(T_i)_0^0 + \sum_{M=\pm1,0} b^M\,(T_i)_M^1 + \sum_{M=\pm2,\pm1,0} c^M\,(T_i)_M^2, \qquad (i = 1, 2).$$

In their turn, the matrices T_q^k may be written through the spin operators explicitly [17]

$$T_0^0 = \frac{1}{\sqrt{3}}I, \qquad T_{\pm1}^1 = \mp\tfrac{1}{2}\left(S_x \pm \mathrm{i}S_y\right), \qquad T_0^2 = \sqrt{\tfrac{3}{2}}((S^z)^2 - \tfrac{2}{3}I),$$
$$T_{\pm1}^2 = \mp\tfrac{1}{2}\left[(S_xS_z + S_zS_x) \pm \mathrm{i}\left(S_yS_z + S_zS_y\right)\right],$$
$$T_{\pm2}^2 = \tfrac{1}{2}\left[\left(S^x\right)^2 - \left(S^y\right)^2 \pm \mathrm{i}\left(S_xS_y + S_yS_x\right)\right].$$

The transformation $\exp(H)$ should preserve the symmetry of the Hamiltonian H. Thus, the requirement of invariance gives the most general form

$$\begin{aligned}\exp H_{12} = {} & \alpha_1 \left((T_1)^0_0 \otimes (T_2)^0_0\right) + \alpha_2 \left((T_1)^1_0 \otimes (T_2)^1_0\right) + \alpha_3 \left((T_1)^2_0 \otimes (T_2)^2_0\right) \\ & + \beta \left((T_1)^1_1 \otimes (T_2)^1_{-1} + (T_1)^1_{-1} \otimes (T_2)^1_1\right) + \gamma \left((T_1)^2_2 \otimes (T_2)^2_{-2} + (T_1)^2_{-2} \otimes (T_2)^2_2\right) \\ & + \sigma \left((T_1)^2_1 \otimes (T_2)^2_{-1} + (T_1)^2_{-1} \otimes (T_2)^2_1\right) \end{aligned} \tag{4}$$

with a new set of coupling parameters $\alpha_1, \alpha_2, \alpha_3, \beta, \gamma, \sigma$. For the Hamiltonian (2) the above formula gives

$$\exp H_{12} = \begin{pmatrix} A_{12} & 0 & 0 & 0 & 0 & 0 & 0 & 0 & 0 \\ 0 & B_{12} & 0 & C_{12} & 0 & 0 & 0 & 0 & 0 \\ 0 & 0 & D_{12} & 0 & F_{12} & 0 & G_{12} & 0 & 0 \\ 0 & C_{12} & 0 & B_{12} & 0 & 0 & 0 & 0 & 0 \\ 0 & 0 & F_{12} & 0 & E_{12} & 0 & F_{12} & 0 & 0 \\ 0 & 0 & 0 & 0 & 0 & B_{12} & 0 & C_{12} & 0 \\ 0 & 0 & G_{12} & 0 & F_{12} & 0 & D_{12} & 0 & 0 \\ 0 & 0 & 0 & 0 & 0 & C & 0 & B_{12} & 0 \\ 0 & 0 & 0 & 0 & 0 & 0 & 0 & 0 & A_{12} \end{pmatrix}, \tag{5}$$

where the matrix elements are $A_{12} \equiv \alpha_1/3 + \alpha_2/2 + \alpha_3/6$, $B_{12} \equiv \alpha_1/3 - \alpha_3/3$, $C_{12} \equiv -\beta/2 - \sigma/2$, $D_{12} \equiv \alpha_1/3 - \alpha_2/2 + \alpha_3/6$, $E_{12} \equiv \alpha_1/3 + 2\alpha_3/3$, $F_{12} \equiv -\beta/2 + \sigma/2$, $G_{12} \equiv \gamma$.

Similarly, we obtain the closed expression for the expansion of $\mathrm{Tr}_3 \exp H_{123}$ akin to that of $\exp H_{12}$ where the coefficients in the expansion (4) are functions of the parameters coming into H_{123} (see appendix B for details).

To calculate the exponentials we will diagonalize numerically the 9×9 and 27×27 matrices associated with H_{12} and H_{123}. By using

$$\exp H_{12} = U_{12} \exp(H^{\mathrm{D}}_{12}) U^{\dagger}_{12}, \qquad \exp H_{123} = U_{123} \exp(H^{\mathrm{D}}_{123}) U^{\dagger}_{123},$$

where U_{12}, U_{123} are the unitary matrices turning H_{12}, H_{123} into the diagonal forms $H^{\mathrm{D}}_{12}, H^{\mathrm{D}}_{123}$, we can find numerically $\exp H_{12}$ and $\exp H_{123}$ as functions of corresponding coupling parameters. The same matrix structure (5) of $\exp H_{12}$ and $\mathrm{Tr}_3 \exp H_{123}$ is supported by numerical calculation. The numerical procedure produces a set $\{\alpha_1, \alpha_2, \alpha_3, \beta, \gamma, \sigma\}$ for $\exp H_{12}$, and $\{\bar{\alpha}_1, \bar{\alpha}_2, \bar{\alpha}_3, \bar{\beta}, \bar{\gamma}, \bar{\sigma}\}$ for $\mathrm{Tr}_3 \exp H_{132}$. To obtain the required RG equations we impose

$$\alpha_1 = A_{12} + B_{12} + D_{12} = \bar{A}_{12} + \bar{B}_{12} + \bar{D}_{12} = \bar{\alpha}_1, \tag{6}$$

$$\alpha_2 = A_{12} - D_{12} = \bar{A}_{12} - \bar{D}_{12} = \bar{\alpha}_2, \tag{7}$$

$$\beta = -C_{12} - F_{12} = -\bar{C}_{12} - \bar{F}_{12} = \bar{\beta} \tag{8}$$

and

$$\begin{aligned} & \alpha_3 = E_{12} - B_{12} = \bar{E}_{12} - \bar{B}_{12} = \bar{\alpha}_3, \qquad \gamma = G_{12} = \bar{G}_{12} = \bar{\gamma}, \\ & \sigma = F_{12} - C_{12} = \bar{F}_{12} - \bar{C}_{12} = \bar{\sigma}. \end{aligned} \tag{9}$$

The number of these equations exceeds the number of interactions that enter into the Hamiltonian (2) because all possible bilinear couplings between terminal sites come into play. Thus, in order to carry out the RG decimation we retain the three equations (6)–(8) which implicitly determine K_s, Δ_s and K'_0 as functions of (K_1, Δ_1), (K_2, Δ_2). This set of equations is a counterpart of RG relations for the case of $S = 1/2$ (see equations (12) in [14]).

Now, we have to chose an appropriate hierarchical lattice. We take one of the simplest cells, conserving a point symmetry of the full lattice, with 6 sites and 6 bonds, as depicted in figure 2. We then impose that the correlation function between the two terminal sites 3 and 6

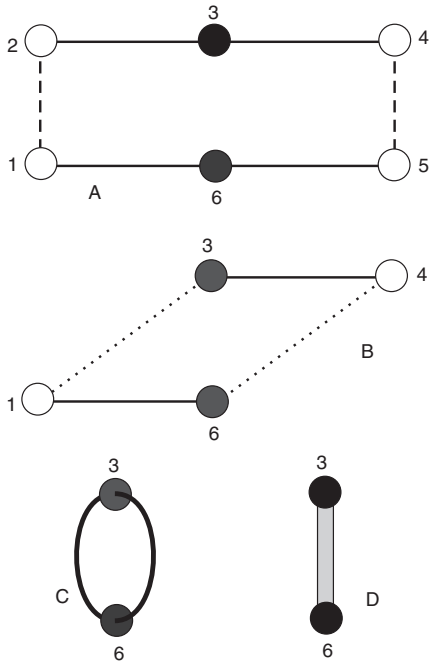

Figure 2. Two-terminal graph used for renormalization purposes.

of the original and renormalized graphs are preserved. At the first step we apply decimation, the spins 1 and 3 (or 4 and 6) survive, whereas the spins 2 and 5 are removed. At the second step the decimation procedure is repeated removing the spins 1 and 4. Finally, to obtain the renormalized parameters we apply Migdal–Kadanoff bond moving, combining the 'pieces' in parallel, which leads to the recursion relations

$$\begin{aligned}(K_S, \Delta_S) &= R_S\,(K_2, \Delta_2; K_1, \Delta_1)\,,\\ (K'_S, \Delta'_S) &= R_S\,(K_S, \Delta_S; K_1, \Delta_1)\,,\\ (K_p, \Delta_p) &= 2(K'_S, \Delta'_S).\end{aligned} \tag{10}$$

We have evaluated numerically the renormalization transformation from the original set of coupling parameters to the set of renormalized parameters. Critical points are then evaluated as non-trivial fixed points of the above relations which can be rewritten as the composite function

$$\left(K_p, \Delta_p\right) = 2R_S\,(R_S\,(K_1, \Delta_1; K_2, \Delta_2)\,; K_1, \Delta_1)\,. \tag{11}$$

Unlike in the case of $S = 1/2$, we cannot obtain RG relations explicitly. Instead, we briefly outline the numerical procedure. Input fixed parameters are the ratio of interchain to intrachain coupling $C_1 = J'_{\mathrm{AF}}/J_{\mathrm{AF}}$ and the anisotropic parameter $\Delta = \Delta_1$; in addition $\Delta_2 = C_1\Delta$ (the feature of anisotropy is the same both for the intrachain and interchain couplings). At a given starting value K_{1i} of the intrachain coupling (then the interchain coupling is $K_{2i} = C_1 K_{1i}$) we apply two successive decimation steps to produce a renormalized coupling K'_S. During each of the steps we solve equations (6)–(8) using the standard routine for non-linear systems of equations [18]. Then, we double the result obtained after these transformations to get a final value K_{f} depending on the starting value K_{1i}. To complete we find a fixed point K_{c} of the equation $K_{1i} = K_{\mathrm{f}}(K_{1i})$ by using the bisection method.

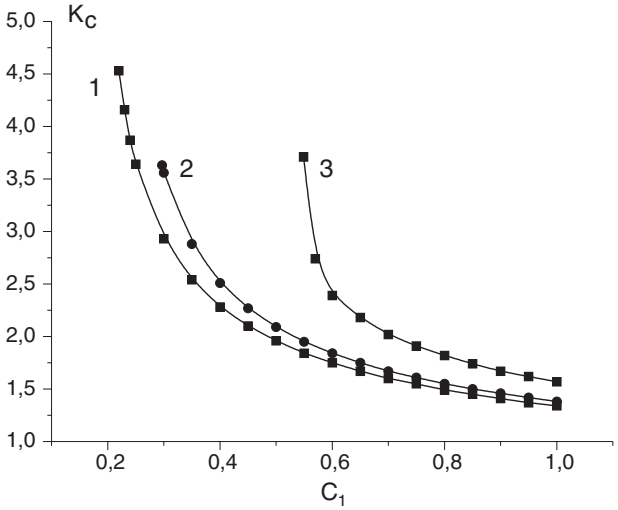

Figure 3. Critical inverse temperature (K_c) versus $C_1 = J'_{AF}/J_{AF}$ found from the RG recursion relations for different anisotropy: $\Delta = 1.0$ (1), $\Delta = 0.8$ (2), $\Delta = 0.6$ (3).

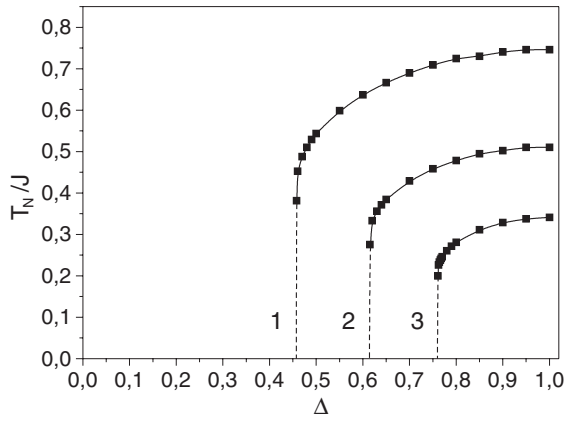

Figure 4. Néel temperature T_N versus Δ phase diagram for different values of the $C_1 = J'_{AF}/J_{AF}$ ratio: 1.0 (1); 0.5 (2); 0.3 (3). The region above (below) the critical line represents the disordered (ordered) phase. The dotted lines are guides to the eye.

3. Results

The critical inverse temperature $K_c = 1/T_c$ as a function of C_1 for several Δ values is presented in figure 3. As seen, the critical temperature rapidly decreases when the interchain coupling becomes weaker. Our results for the critical temperature as a function of the anisotropy Δ are shown in figure 4. The universality class for the whole critical curve is the same as for the Ising model. In contrast to some RSRG calculations for $S = 1/2$, the phase diagrams for ferromagnetic and antiferromagnetic models are the same: the critical temperature reaches zero at a critical value of Δ, Δ_c, which is greater than zero. The weaker the interchain coupling, the stronger the quantum fluctuations. So, as one might expect, the Δ_c value is larger if the C_1 shifts to lower values.

For the lowest temperatures at which we could work, we have observed no sign of the reentrant behaviour found in some previous RSRG treatments. The Néel temperature behaves as

$$T_N \sim \frac{1}{\ln(\Delta - \Delta_c)}$$

near $\Delta = \Delta_c$, which agrees with the result found for the case $S = 1/2$. Our calculation cannot be carried out down to $T = 0$; therefore we cannot make any definite conclusions about the ground state of the model. The scaling law holds for different values of the ratio of interchain to intrachain coupling (figure 5). In [19, 20], the logarithmic dependence of T_N and T_c with respect to $\Delta - \Delta_c$ is established using scaling arguments with $\Delta_c = 0$. Recent quantum Monte Carlo results [4] for the anisotropic 2D $S = 1/2$ Heisenberg model have shown that it develops an ordered low-temperature phase even for very small anisotropies $\Delta \sim 10^{-3}, 10^{-2}$. The latter gives strong evidence of large values of a critical anisotropy which is an artifact of the real-space renormalization approach.

At this point it is worthwhile comparing our results with those from RSRG calculations for the antiferromagnetic AH model of $S = 1/2$ on a square lattice. These RSRG analyses lead to non-equivalence between the criticality of the ferromagnetic (F) and antiferromagnetic (AF) models, a reentrant behaviour in the (T, Δ) diagram [10, 11].

It is well known that in classical spin models, such as the Ising or classical Heisenberg models, on bipartite lattices the critical temperature is the same for ferromagnetic exchange (Curie temperature) as for antiferromagnetic exchange (Néel temperature). This is a direct consequence of the free energy being an even function of the exchange parameter. However, for the quantum spin-1/2 Heisenberg model the Curie and Néel temperatures are unequal [21]. Recently, this question has been reinvestigated using high-temperature series expansions for the spin-1/2, 1 and 3/2 Heisenberg ferromagnet and antiferromagnet in three dimensions [22]. The difference between the temperatures decreases rapidly with increasing spin-S. In some quantum systems, such as the quantum spin-1/2 XY and transverse Ising models, an isomorphism between the criticality of the F and AF cases is observed [23]. Critical properties of the quantum spin-1/2 2D Heisenberg model with anisotropic interaction treated by the Green function technique yields $T_c = T_N$ for all values of the anisotropy parameter [24, 25]. RSRG methods give contradictory results of the problem because of underlying approximations whose effects are hard to control in a systematic way. In [10, 11] this was obtained by the RG approach $T_N < T_c$ for the 2D anisotropic Heisenberg limit $0 \leqslant \Delta < 1$ due to a special choice of the hierarchical lattice approximating a square one. The critical temperature T_c for the 2D ferromagnetic spin-1/2 anisotropic Heisenberg model tends gradually to zero when decreasing the anisotropy parameter Δ, i.e. $T_c = 0$ in the isotropic Heisenberg limit $\Delta = 0$ in accordance with the Mermin–Wagner theorem [26]. The results for the antiferromagnetic exchange are very similar to the $S = 1/2$ case, where there is no long-range Néel order for the anisotropy parameter $\Delta < \Delta_c$. The question is not yet settled, and more work is needed to get these points on firmer ground.

An observation of reentrant behaviour for the spin-1/2 antiferromagnetic AH model on the square lattice has been reported by some authors [10, 11]. This result suggests that there is an ordered phase at relatively high temperature but not at very low temperature. A full understanding of this phenomena is still lacking, but it is most likely that the reentrant behaviour is an artifact of the RSRG method. In [27] the authors attribute the reentrance to the effect of finite size in the renormalization, and for larger clusters it should be absent.

In conclusion, the real-space renormalization group is employed to study the anisotropic Heisenberg model of spin $S = 1$ on a honeycomb lattice with two kinds of antiferromagnetic coupling. We calculate dependencies of the critical temperature on the parameters of the

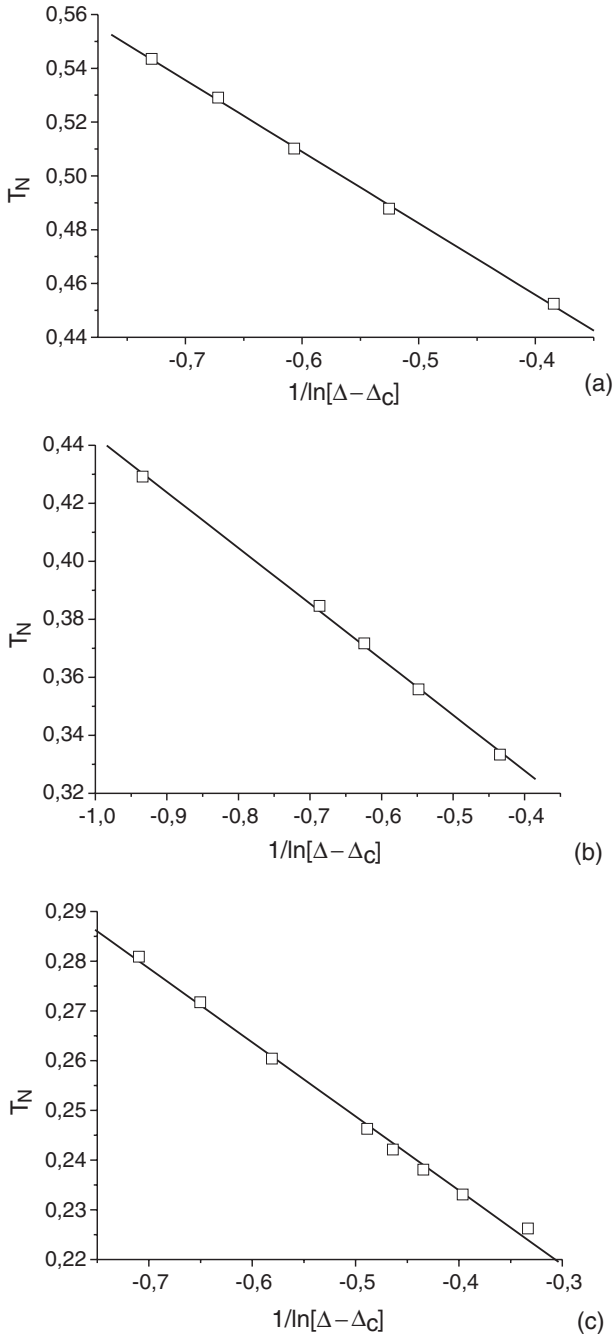

Figure 5. Phase diagram T_N versus Δ for small T_N near Δ_c: $C_1 = 1.0$ and $\Delta_c \simeq 0.46$ (a), $C_1 = 0.5$ and $\Delta_c \simeq 0.62$ (b), $C_1 = 0.3$ and $\Delta_c \simeq 0.76$ (c).

magnetic anisotropy, and on the ratio of interchain and intrachain exchange interactions. The entire critical line is found to belong to the universality class of the Ising model. In accordance with the early RSRG predictions for the antiferromagnetic AH model of spin

$S = 1/2$ on a square lattice, our calculations recover the existence of large finite critical anisotropy Δ_c, which should be considered as an artifact of the real-space renormalization technique.

Acknowledgments

We would like to thank Professor M V Sadovskii for discussions. We acknowledges partial financial support from grant NREC-005 of the US CRDF (Civilian Research and Development Foundation).

Appendix A

The polarization matrices for spin $S = 1$ have the explicit form

$$T_{00} = \frac{1}{3}\begin{pmatrix} 1 & 0 & 0 \\ 0 & 1 & 0 \\ 0 & 0 & 1 \end{pmatrix}, \quad T_{11} = -\frac{1}{\sqrt{2}}\begin{pmatrix} 0 & 1 & 0 \\ 0 & 0 & 1 \\ 0 & 0 & 0 \end{pmatrix}, \quad T_{1-1} = \frac{1}{\sqrt{2}}\begin{pmatrix} 0 & 0 & 0 \\ 1 & 0 & 0 \\ 0 & 1 & 0 \end{pmatrix},$$
$$T_{10} = \frac{1}{\sqrt{2}}\begin{pmatrix} 1 & 0 & 0 \\ 0 & 0 & 0 \\ 0 & 0 & -1 \end{pmatrix}, \quad T_{20} = \frac{1}{\sqrt{6}}\begin{pmatrix} 1 & 0 & 0 \\ 0 & -2 & 0 \\ 0 & 0 & 1 \end{pmatrix}, \quad T_{21} = \frac{1}{\sqrt{2}}\begin{pmatrix} 0 & -1 & 0 \\ 0 & 0 & 1 \\ 0 & 0 & 0 \end{pmatrix},$$
$$T_{2-1} = \frac{1}{\sqrt{2}}\begin{pmatrix} 0 & 0 & 0 \\ 1 & 0 & 0 \\ 0 & -1 & 0 \end{pmatrix}, \quad T_{22} = \begin{pmatrix} 0 & 0 & 1 \\ 0 & 0 & 0 \\ 0 & 0 & 0 \end{pmatrix}, \quad T_{2-2} = \begin{pmatrix} 0 & 0 & 0 \\ 0 & 0 & 0 \\ 1 & 0 & 0 \end{pmatrix}.$$

Appendix B

We first take care of H'_{12} and express it in the basis $|M_1 M_2\rangle$. In this basis H'_{12} becomes

$$H'_{12} = \begin{pmatrix} K'_0 + K_S & 0 & 0 & 0 & 0 & 0 & 0 & 0 & 0 \\ 0 & K'_0 & 0 & W_S & 0 & 0 & 0 & 0 & 0 \\ 0 & 0 & K'_0 - K_S & 0 & W_S & 0 & 0 & 0 & 0 \\ 0 & W_S & 0 & K'_0 & 0 & 0 & 0 & 0 & 0 \\ 0 & 0 & W_S & 0 & K'_0 & 0 & W_S & 0 & 0 \\ 0 & 0 & 0 & 0 & 0 & K'_0 & 0 & W_S & 0 \\ 0 & 0 & 0 & 0 & W_S & 0 & K'_0 - K_S & 0 & 0 \\ 0 & 0 & 0 & 0 & 0 & W_S & 0 & K'_0 & 0 \\ 0 & 0 & 0 & 0 & 0 & 0 & 0 & 0 & K'_0 + K_S \end{pmatrix}$$

where $W_S = K_S(1 - \Delta_S)$.

Performing the same calculation for H_{123}, now using the basis $|M_1 M_3 M_2\rangle$, we arrive at a 27×27 matrix which has 4 independent blocks of size 9×9

$$H_{123} = \begin{pmatrix} A_1 & B_2 & 0 \\ B_1 & A_2 & B_2 \\ 0 & B_1 & A_3 \end{pmatrix},$$

where the $9 \times 9 A_1$, B_1, B_2, A_2 and A_3 are given by

$$A_1 = \begin{pmatrix} K_1+K_2 & 0 & 0 & 0 & 0 & 0 & 0 & 0 & 0 \\ 0 & K_1 & 0 & W_2 & 0 & 0 & 0 & 0 & 0 \\ 0 & 0 & K_1-K_2 & 0 & W_2 & 0 & 0 & 0 & 0 \\ 0 & W_2 & 0 & 0 & 0 & 0 & 0 & 0 & 0 \\ 0 & 0 & W_2 & 0 & 0 & 0 & W_2 & 0 & 0 \\ 0 & 0 & 0 & 0 & 0 & 0 & 0 & W_2 & 0 \\ 0 & 0 & 0 & 0 & W_2 & 0 & -K_1-K_2 & 0 & 0 \\ 0 & 0 & 0 & 0 & 0 & W_2 & 0 & -K_1 & 0 \\ 0 & 0 & 0 & 0 & 0 & 0 & 0 & 0 & -K_1+K_2 \end{pmatrix},$$

$$A_2 = \begin{pmatrix} K_2 & 0 & 0 & 0 & 0 & 0 & 0 & 0 & 0 \\ 0 & 0 & 0 & W_2 & 0 & 0 & 0 & 0 & 0 \\ 0 & 0 & -K_2 & 0 & W_2 & 0 & 0 & 0 & 0 \\ 0 & W_2 & 0 & 0 & 0 & 0 & 0 & 0 & 0 \\ 0 & 0 & W_2 & 0 & 0 & 0 & W_2 & 0 & 0 \\ 0 & 0 & 0 & 0 & 0 & 0 & 0 & W_2 & 0 \\ 0 & 0 & 0 & 0 & W_2 & 0 & -K_2 & 0 & 0 \\ 0 & 0 & 0 & 0 & 0 & W_2 & 0 & 0 & 0 \\ 0 & 0 & 0 & 0 & 0 & 0 & 0 & 0 & K_2 \end{pmatrix},$$

$$A_3 = \begin{pmatrix} -K_1+K_2 & 0 & 0 & 0 & 0 & 0 & 0 & 0 & 0 \\ 0 & -K_1 & 0 & W_2 & 0 & 0 & 0 & 0 & 0 \\ 0 & 0 & -K_1-K_2 & 0 & W_2 & 0 & 0 & 0 & 0 \\ 0 & W_2 & 0 & 0 & 0 & 0 & 0 & 0 & 0 \\ 0 & 0 & W_2 & 0 & 0 & 0 & W_2 & 0 & 0 \\ 0 & 0 & 0 & 0 & 0 & 0 & 0 & W_2 & 0 \\ 0 & 0 & 0 & 0 & W_2 & 0 & K_1-K_2 & 0 & 0 \\ 0 & 0 & 0 & 0 & 0 & W_2 & 0 & K_1 & 0 \\ 0 & 0 & 0 & 0 & 0 & 0 & 0 & 0 & K_1+K_2 \end{pmatrix},$$

$$B_2 = B_1^T = \begin{pmatrix} 0 & 0 & 0 & 0 & 0 & 0 & 0 & 0 & 0 \\ 0 & 0 & 0 & 0 & 0 & 0 & 0 & 0 & 0 \\ 0 & 0 & 0 & 0 & 0 & 0 & 0 & 0 & 0 \\ W_1 & 0 & 0 & 0 & 0 & 0 & 0 & 0 & 0 \\ 0 & W_1 & 0 & 0 & 0 & 0 & 0 & 0 & 0 \\ 0 & 0 & W_1 & 0 & 0 & 0 & 0 & 0 & 0 \\ 0 & 0 & 0 & W_1 & 0 & 0 & 0 & 0 & 0 \\ 0 & 0 & 0 & 0 & W_1 & 0 & 0 & 0 & 0 \\ 0 & 0 & 0 & 0 & 0 & W_1 & 0 & 0 & 0 \end{pmatrix},$$

where $W_1 = K_1(1 - \Delta_1)$ and $W_2 = K_2(1 - \Delta_2)$.

References

[1] Hosokoshi Y, Nakazawa Y, Inoue K, Takizawa K, Nakano H, Takahashi M and Goto T 1999 *Phys. Rev.* B **60** 12924

[2] Ho T L and Yip S K 2000 *Phys. Rev. Lett.* **84** 4031

[3] Yip S 2003 *J. Phys.: Condens. Matter* **15** 4583

[4] Cuccoli A, Roscilde T, Tognetti V, Vaia R and Verrucchi P 2003 *Phys. Rev.* B **67** 104414

[5] Niemeijer Th and van Leeuwen J M J 1973 *Phys. Rev. Lett.* **31** 1412

[6] Kadanoff L P and Houghton A 1975 *Phys. Rev.* B **11** 377

[7] Rogiers J and Dekeyser R 1976 *Phys. Rev.* B **13** 4886

[8] Stella A L and Toigo F 1978 *Phys. Rev.* B **17** 2343
[9] Brower R C, Kuttner F, Nauenberg M and Subbarao K 1977 *Phys. Rev. Lett.* **38** 1231
[10] de Souza A M C 1993 *Phys. Rev.* B **48** 3744
[11] Branco N S and de Sousa J R 2000 *Phys. Rev.* B **62** 5742
[12] Sznajd J 2001 *Phys. Rev.* B **63** 184404
[13] Suzuki M and Takano H 1979 *Phys. Lett.* A **69** 426
Takano H and Suzuki M 1981 *J. Stat. Phys.* **26** 635
[14] Mariz A M, Tsallis C and Caride A O 1985 *J. Phys. C: Solid State Phys.* **18** 4189
[15] Migdal A A 1975 *Zh. Eksp. Teor. Fiz.* **69** 810
Migdal A A 1975 *Sov. Phys.—JETP* **42** 413 (Engl. Transl.)
Migdal A A 1975 *Zh. Eksp. Teor. Fiz.* **69** 1457
Migdal A A 1975 *Sov. Phys.—JETP* **42** 743 (Engl. Transl.)
[16] Kadanoff L P 1976 *Ann. Phys.* **100** 359
[17] Varshalovich D A, Moskalev A N and Khersonskii V K 1988 *Quantum Theory of Angular Momentum* (Singapore: World Scientific)
[18] Press W H, Flammery B P, Teukolsky S A and Vetterling W T 1992 *Numerical Recipes in C: The Art of Scientific Computing* (Cambridge: Cambridge University Press)
[19] Ding H-Q 1990 *J. Phys.: Condens. Matter* **2** 7979
[20] Aplesnin S S 1998 *Phys. Solid State* **207** 491
[21] Rushbrooke G S and Wood P J 1963 *Mol. Phys.* **6** 409
[22] Oitmaa J and Zheng W 2004 *J. Phys.: Condens. Matter* **16** 8653
[23] de Souza J R and Araujo I G 1999 *J. Magn. Magn. Mater.* **202** 231
[24] Singh R P, Tao Z C and Singh M 1992 *Phys. Rev.* B **46** 1244
[25] Liu B G 1990 *Phys. Rev.* B **41** 9563
[26] Mermin N D and Wagner H 1966 *Phys. Rev. Lett.* **17** 1133
[27] de Souza J R and Araujo I G 2000 *Phys. Lett.* A **272** 333